A NEW APPROACH TO MODEL DETERMINATION OF LARGE FLEXIBLE SPACE SYSTEMS

F.Y. Hadaegh, D.S. Bayard, Y. Yam and E. Mettler

Jet Propulsion Laboratory
California Institute of Technology
4800 Oak Grove Drive
Pasadena, California 91109

ABSTRACT

The product moment matrix (PMM) is used for the estimation of linear model order for flexible space structures from the input-output data. A new automated frequency domain identification methodology is presented and experimentally verified for on-orbit determination of transfer functions. The identification process is initiated by applying stochastic inputs to the system giving rise to a nonparametric spectral estimate of the structural parameters. The PMM algorithm obtains an initial estimate of the model order and together with the initial parameter estimates, they provide an initializing transfer function. The system transfer function is then obtained by curve fitting the spectral estimates to a rational transfer function. This approach makes efficient use of the actuators and sensors already available on the system for control applications and also demonstrates that on-orbit identification capability is a realistic objective for the future space systems.

1. Introduction

The mathematical modeling and identification of large flexible space systems have been challenging tasks for several decades. The models for such systems should predict the behavior of the actual system under restricted experimental conditions. Furthermore, when correlated and tested against the actual data, they should explain the observed behavior of the system through post-mission data analysis. In practice, the identification problem is often separated into two parts: a) determination of the order for a linear model and b) estimation of the parameter values of the resulting model. Clearly, in a linear system the model structure is determined by the choice of the order. Hence, an incorrect structural assumption may manifest itself in biased parameter estimates or may even lead to erroneous conclusions on the results of the identification process (e.g., a large model order leads to over parameterizations and identifiability problems; where as a small order may result in a large bias in parameter estimates). This is of particular interest in the case of on-orbit identification where model parameters have physical significance and the accuracy of the parameter estimate is the primary objective of the system identification experiment. On- orbit system identification enables on-line design of robust, high performance control systems. This capability has the potential to improve the performance robustness and control accuracy under operational constraints and environmental uncertainties far beyond that attainable by using nominal system descriptions obtained from ground testing and analysis alone.

This paper presents a new frequency domain system identification architecture designed to operate with a high degree of autonomy and to restrict the "human in the loop" requirements. This includes an automated estimation of model order in the presence of measurement noise; the main subject for discussion in this paper. Major theoretical and experimental developments associated with this approach are discussed in [10]. Different techniques for model order determination have been studied [1-9]. They include fit-error statistics [1], Akaike's criterion [2], Kalman filtering [3], likelihood ratio test [4], methods based on pole-zero cancellation [7], statistical F-test [8], and Parzen's criteria [9]. These methods are often estimation based oriented and utilize statistical methods for extracting information about a system model from the observed data. They often require normality assumption on the measurement noise and furthermore, they involve processing of large volumes of data. Here, the product moment matrix [5] approach is chosen for a variety of reasons and in each case it proves advantageous over alternate methods. For example, the PMM requires no a priori assumption on the model parameterization and form and it requires no knowledge of density or distribution functions of unknown parameters or data. This technique is applicable to both deterministic and stochastic systems. Finally, the PMM algorithm is robust with respect to uncertainties and it produces meaningful results even in the presence of significant additive measurement noise. A brief discussion of the PMM algorithm follows.

2. The Product Moment Matrix

The idea behind the PMM approach is to analyze the correlation function of the input-output variables for a linear model of changing structure. This will subsequently lead to a pronounced dynamic behavior around the "true" order of the system. This behavior may be observed through the determinants or eigenvalues of the product moment matrix with elements constructed as follows.

Let $\{u_k\}$ and $\{y_k\}$ be a set of observations of input and output respectively (data) which are contaminated by measurement noise. Let us also assume that the input signal is sufficiently rich such that it persistently excites all system modes of interest. A linear system of order n has a system function which is given by

$$H(z) = \frac{Y(z)}{U(z)} = \frac{\sum_{i=1}^{n} \theta_{2i-1} z^{-i}}{1 - \sum_{i=1}^{n} \theta_{2i} z^{-i}} \tag{1}$$

letting

$$\theta^T(n) = [\theta_1, \ldots, \theta_{2n}] \tag{2}$$

and

$$\wedge^T(k,n) = [u_{k-1}, y_{k-1}, u_{k-2}, y_{k-2}, \ldots, u_{k-n}, y_{k-n}] \tag{3}$$

Then in time-domain, the measured system response is given by

$$y_k = \theta^T(n) \wedge (k,n) \tag{4}$$

For N measurements, the "generalized Hankel matrix" $H(N)$ is as follows.

$$H(N) = \begin{pmatrix} y_o & y_1 & \cdots & y_{N-1} \\ y_1 & y_2 & \cdots & y_N \\ \vdots & \vdots & & \\ y_{N-1} & y_N & & y_{2N-2} \end{pmatrix} \triangleq y_{i+j-2} \qquad i,j > 0 \tag{5}$$

Similarly, the generalized Hankel matrix for the $N \times N$ block matrices formed out of the shifted sequence $y_{k+\ell}$ will be

$$H(N) = [y_{i+j+\ell-2}]$$

If a finite-dimensional realization for the system exists, denoting n^* as the rank of its minimal realization, then [21]

$$n^* = \text{ Rank } H(N) \tag{6}$$

Since n^* is the dimension of a **minimal** realization of the system which is unknown, it will subsequently be referred to as the "true" order of the system. Note also that the ordering of components in the vectors $\wedge(k,n)$ and $\theta(n)$ are such that for a higher-order model, additional components are simply added to the end of these vectors. The product moment matrix of the system is defined by:

$$Q[n,N] \equiv Q_n \triangleq \frac{1}{N} \sum_{k=1}^{N} \wedge(k,n) \wedge^T (k,n)$$

$$= \frac{1}{N} \begin{pmatrix} \sum_{k=1}^{N} u_{k-1}^2 & \sum_{k=1}^{N} u_{k-1}y_{k-1} & \cdots & \sum_{k=1}^{N} u_{k-1}y_{k-n} \\ \sum_{k=1}^{N} y_{k-1}u_{k-1} & \sum_{k=1}^{N} y_{k-1}^2 & \cdots & \sum_{k=1}^{N} y_{k-1}y_{k-n} \\ \vdots & & & \vdots \\ \sum_{k=1}^{N} y_{k-n}u_{k-1} & \sum_{k=1}^{N} y_{k-n}y_{k-1} & \cdots & \sum_{k=1}^{N} y_{k-n}^2 \end{pmatrix} \tag{7}$$

where n is an assumed order for the system and N is the number of data points. If the data is noise free, then Q_n will become singular for all $n > n^*$ [6], and

$$\text{Rank}[Q_n] = \left\{ \begin{matrix} = & 2n \\ = & n+n^* \end{matrix} \right\} \text{for } n \left\{ \begin{matrix} \leq \\ > \end{matrix} \right\} n^* \tag{8}$$

Hence, Q_n has the following properties:

$$\det[Q_n] = \left\{ \begin{matrix} \neq & 0 \\ = & 0 \end{matrix} \right\} \text{for } n \left\{ \begin{matrix} \leq \\ > \end{matrix} \right\} n^* \tag{9}$$

For an arbitrary value of N and an assumed value of n, the ratio

$$D_n = \frac{\det[Q_n]}{\det[Q_{n+1}]} \tag{10}$$

is calculated for succeeding model orders $n+1, \ldots, n^*, \ldots, n_{\max}$. If the value of D_n exhibits a distinct increase compared to D_{n-1}, then n corresponds approximately to n^*. In the presence of noise however, the $\text{Det}[Q_n]$ is usually non-zero for $n > n^*$.

In practice, where the measurement noise is nonwhite, the enhanced PMM given by

$$\check{Q}_n = Q_n - \sum_n \tag{11}$$

is used. An estimate of $\sum_n$, the measurement noise contributions to the PMM, is obtained by first collecting measurements from the system when the input to the system is identically zero. Denoting the input measurement noise by n_u and the output measurement noise by n_y, then $\sum_n$ is computed as

$$\sum_n = Q_n |\, y = n_y, u = n_u$$

The $\check{Q}$ product moment matrix henceforth referred to as enhanced product moment matrix (EPMM) will reduce to the formulations (7) depending upon the nature of noise in the data. The EPMM, although computationally less efficient, gives a better estimate of the system order in the presence of measurement noise.

An alternative representation of PMM is given as follows:

$$Q_n = E[a_n a_n^T] \tag{12}$$

where

$$a_n^T = [u_0\ y_0\ u_1\ y_1 \ldots u_{n-1} y_{n-1}]$$

and E is the statistical expectation operation. We will refer to Equation (12) as the stochastic representation of PMM and the Equations (7) and (11) as the deterministic representations of PMM.

When the underlying dynamical process is stationary, the correlations have the form:

$$\begin{aligned} E[u_i y_j] &= R_{uy}(j-i) \\ E[u_i u_j] &= R_{uu}(j-i) = R_{uu}(i-j) \\ E[y_i y_j] &= R_{yy}(j-i) = R_{yy}(i-j) \end{aligned} \tag{13}$$

Then by assuming that the process is ergodic, temporal averages are equivalent to ensemble averages, and the product moment matrix given in (7) has the simple analytical form:

$$\lim_{N \to \infty} Q(N,n) = Q_*(n) \tag{14}$$

$$Q_*(n) = \begin{bmatrix} Q_*^{(1,1)} & \ldots & Q_*^{(1,n)} \\ \vdots & & \vdots \\ Q_*^{(n,1)} & \ldots & Q_*^{(n,n)} \end{bmatrix} \tag{15}$$

$$Q_*^{(i,j)} = \begin{bmatrix} R_{uu}(j-i) & R_{yu}(j-i) \\ R_{uy}(j-i) & R_{yy}(j-i) \end{bmatrix} \tag{16}$$

This explicitly gives the product moment matrix without requiring any additional processing of the input and output data. Thus when correlations are available under these circumstances, the product moment matrix can be constructed with considerable fewer arithmetric operations than those required by the deterministic algorithms. The key practical issues are the validity of the assumptions regarding stationarity and ergodicity of the signals and the means for calculating the correlation functions based on finite-time data lengths. A brief description of modeling and identification algorithm architecture and methodology follows.

3. Functional Architecture, Modeling and Identification Description

The functional architecture is outlined schematically in Fig. 1. The flow of the various processes is automated and controlled from a single human operator as described below.

a) **The plant $p(e^{j\omega T})$ is excited by one of a variety of possible input excitations $u(kT)$ of both stochastic (i.e., wideband or narrowband) or deterministic (i.e., sine-dwell) types giving rise to plant output $y(kT)$.**

The wideband input is simply a random number generator which produces independent uniformly distributed variates. The narrowband input is produced by digitally filtering the wideband input according to desired spectral characteristics. The capability for on-line digital filter design is provided as part of the system software. The sine-dwell inputs are piecewise constant approximations to true sinusoids, consistent with the sample-and-hold discretization.

Wideband signals are also constructed artificially using a technique which we call data composition. This is done by designing a bank of bandpass filters to cover a wideband portion of the frequency axis, and then running a separate experiment for each bandpass process. The input and output sequences from all bandpass experiments are then composed (i.e., added together respectively) to give data for what is effectively a single wideband experiment. The realization of such a wideband excitation in a single experiment would otherwise be impossible due to actuator power constraints.

b) **The plant transfer function is identified nonparametrically by spectral estimation (in the case of stochastic inputs) and by gain and phase estimation in the case of sine-dwell inputs.**

For experiments using stochastic input excitation, spectral estimation is invoked to compute the correlations R_{uu}, R_{yy}, R_{uy} and spectral estimates P_{uu}, P_{yy}, P_{uy} from the input and output data, as well as the plant transfer function estimate from the cross-spectral estimate $h = P_{uy}/P_{uu}$.

For experiments using sine-dwell input excitation, the gain, phase, real and imaginary parts of $p(e^{j\omega T})$ at sine-dwell frequencies are determined in real-time using a recursive least squares estimator with exponential forgetting factor. This approach is particularly well suited to provide accurate estimation using sampled-data sinusoidal responses and to operate in the presence of low frequency resonances. The time constant for the forgetting factor is typically chosen to be several cycles of the sine-dwell response. The sine-dwell estimates of plant gain, phase and real and imaginary parts of $p(e^{j\omega T})$ over several frequencies can be stored for later use by the transfer function curve fitting routine.

c) **Anticipating parametric curve fitting to follow, the model order is estimated using a product moment matrix (PMM) test.**

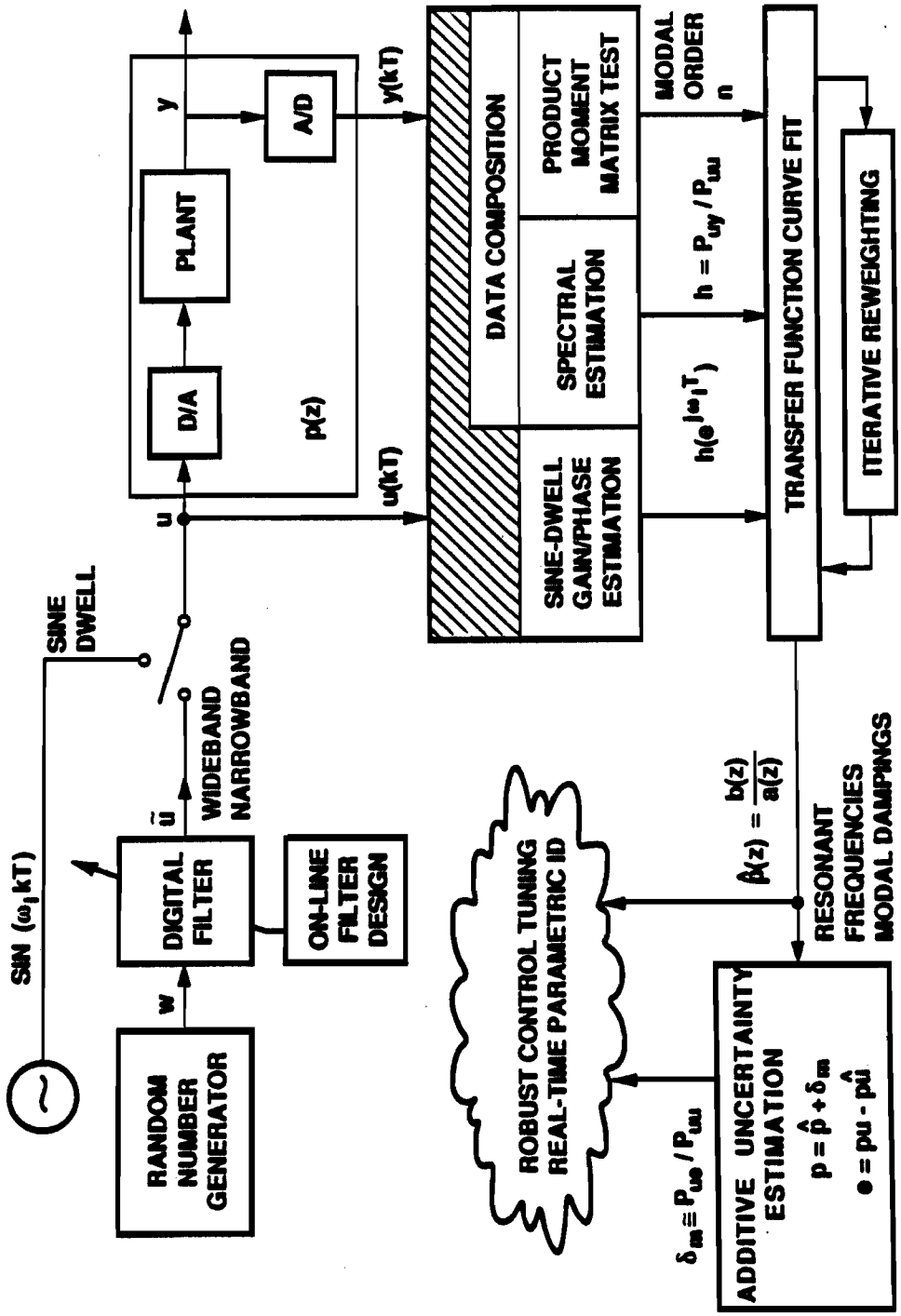

Figure 1. Functional Architecture of System ID Experiment.

To overcome much of the guessing and "human in the loop" efforts typically associated with model order determination task, an initial estimate of the model order is obtained by PMM test, and then followed by a search for the optimal order in the vicinity of this estimate by a sequence of curve fits with varying orders. The quality of each fit is judged by the output error profile.

The PMMD operates on raw data, and generates the PMM directly from the plant input and output. The PMMS assumes statistical stationarity for the underlying process and generates the PMM from the smoothed estimates of the auto and cross covariances produced from the spectral estimation software.

d) **The plant is identified parametrically by fitting transfer function coefficients to the nonparametric data. Model order is determined by a sequential search starting at the PMM estimate.**

A parametric transfer function estimate $\hat{p}$ is determined by curve fitting the coefficients of a rational transfer function to the nonparametric frequency domain data. The data in this case is specified to be the spectral estimate $h = P_{uy}/P_{uu}$ and/or sine-dwell estimates. The model order is determined by successively increasing the number of modes in the curve fit, starting at the PMM estimate, until an adequate output error profile is observed. The curve fit involves the use of a least squares algorithm with a special iterative reweighting technique which removes high frequency emphasis (typically associated with equation error methods), and assures minimum variance estimation of the transfer function coefficients. Resonant frequencies and damping estimates are automatically found by robustly factorizing the plant denominator polynomial with a special purpose routine.

e) **The output error is determined to characterize the quality of the parametric transfer function estimate, and for later use in robust control analysis and design.**

The output error $e = pu - \hat{p}u$ is computed by subtracting the predicted output $\hat{y} = \hat{p}u$ from the measured data $y = pu$ and then the additive uncertainty $\delta_m = p - \hat{p}$ is estimated by the cross-spectral estimate $\Delta = P_{ue}/P_{uu}$. The nominal plant transfer function estimate $\hat{p}$ and the estimate Δ of the additive uncertainty δ_m can then be used directly for robust control analysis and design. The motivation and usefulness of using the output error characterization of additive uncertainty, and its role in robust control design is discussed in [10].

4. Testbed Description

Experimental demonstration and verification of modeling and identification software performance was conducted on the JPL/AFAL Flexible Structure Testbed. The design of this 3-D antenna-like structure was adopted as it exhibits many characteristics of a typical large space structure. These include many low frequency modes, densely packed modes, low structural damping, and three-dimensional structural interaction among components.

In this section, a brief description of the testbed facility is given. Detail description can be found in [10]. The main component of the testbed facility is shown in Figure 2. It consists of a central rigid hub to which are attached 12 ribs. The ribs are coupled together by two rings of pretensioned wires.

Functionally, the wires are intended to simulate the coupling effects of a reflective mesh installed over the rib frame in an actual antenna. The ribs are 2.25 m in length. The hub is of radius 0.6 m, making the dish structure 5.7 m in diameter. The tensioning wires are installed in two rings at approximate diameters of 3 m and 4.8 m. As intended to achieve low modal freqencies, the ribs are very flexible. Stand along, they are unable to support their own weight without excessive droop. To prevent structural collapse due to gravity, each rib is supported at two locations along its free length by levitators. Each levitator is constituted by a counterweight attached to the rib with a wire which passes over a low-friction pulley. The support locations were calculated to minimize the rms shape deviation along the rib from the root to tip. The calculations led to supporting the rib at the 40% and 80% points which are 0.9 m and 1.8 m from the rib root, the same locations for coupling wire attachments. A flexible boom is attached to the central axis of the hub and has a mass at its lower end to simulate the feed horn of an antenna of the secondary mirror assembly or an optical system. The original boom length was 3.6 m, but for the convenience of conducting experiment at ground level, a second, 1 m long boom is being used for most of the experiments. The feed mass is 4.5 kg. The hub is mounted to a backup structure via a two-axis gimbal which allows rotational freedom about two perpendicular axes in the horizontal plane. The gimbal bearings support roughly one quarter the weight of the ribs, the entire weight of the hub, boom, and feed, and their respective sensing and actuation devices. Each of the ribs can be excited dynamically by a single rib-root actuator with a lever arm of about 0.3 m from the hub attachment point. Each rib-root actuator consists of a speaker-coil type device which reacts against a mount rigidly attached to the hub. In addition, two speaker-coil type actuators are mounted on the hub to provide controlled torquing about the two gimbal axes. These hub torquers apply linear forces to the hub at its outer circumference to yield the required torques about the axis of rotation. Together, these 14 actuators are capable of controlling all flexible modes of the structure. Each of the 24 levitators is equipped with an incremental optical encoder which measures the relative angular rotation of the levitator pulley. These angular measurements are then translated into the vertical motion of the ribs at the levitator/rib attachment points, relative to the backup structure. Additional linear variable differential transformers (LVDT) sensors are provided to determine the rib displacement measurements at four evenly space rib root actuator locations. Hub angular rotations about the two axes are measured by two rotary variable differential transformers (RVDT) mounted directly at the gimbal bearings.

Figure 2. JPL/AFAL Flexible Structure Testbed.

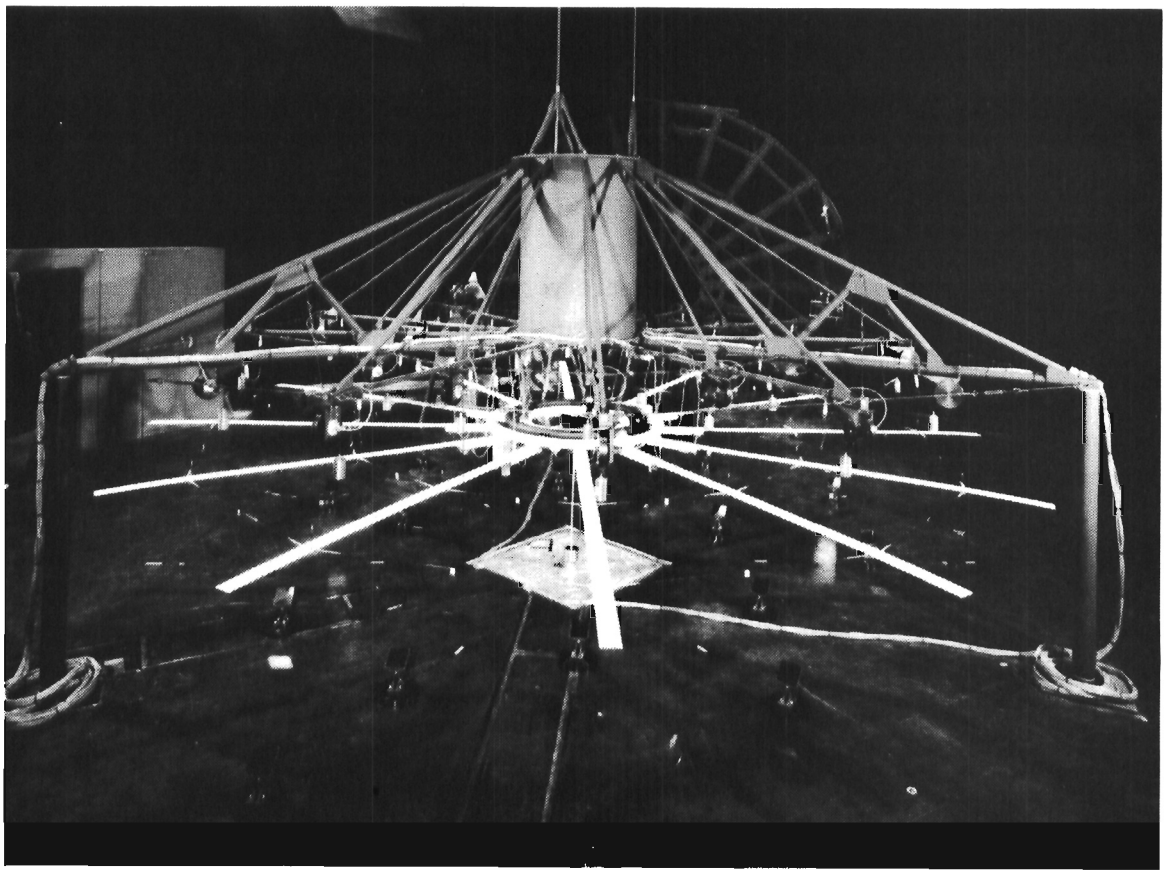

PHOTOGRAPH

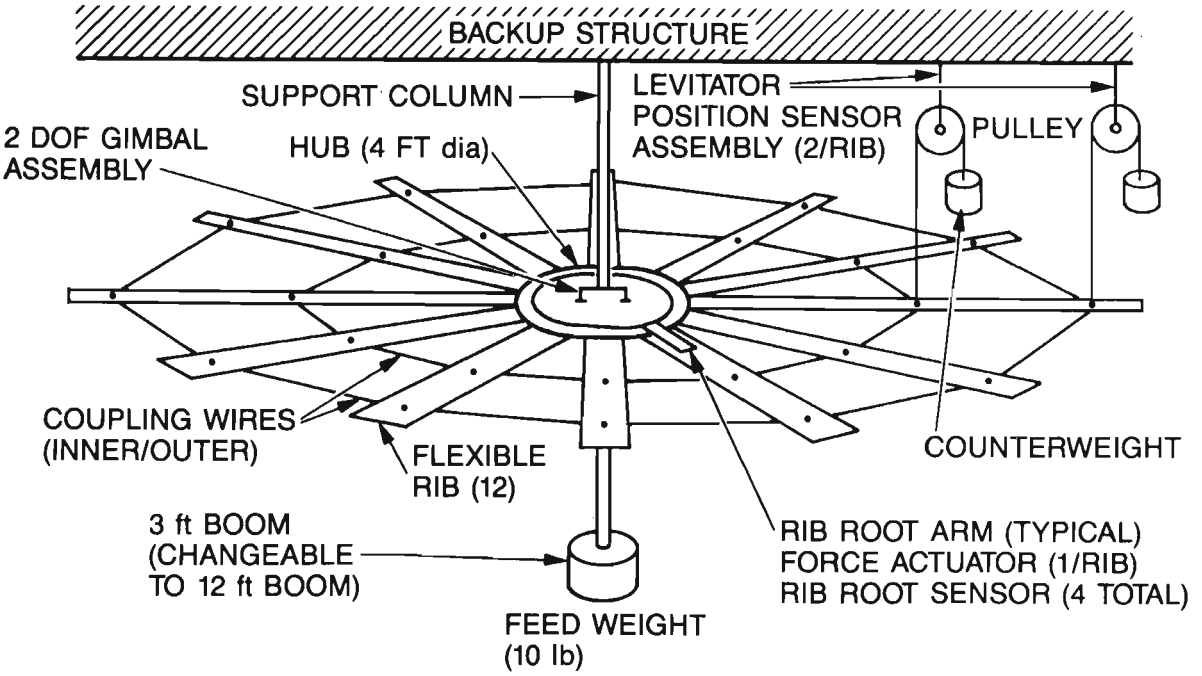

SCHEMATIC

5. Case Study with Experimental Data

Results of a wideband excitation experiment are shown in Figures 3-A to H. The experiment was performed on one of the two hub axes of the JPL/AFAL Flexible Structure Testbed utilizing a collocated hub torquer and an RVDT angular sensor for instrumentation. The sampling frequency was 20 Hz. The experiment run time was 1638.4 sec. Figure A shows the white noise input excitation u uniformly distributed between the range ± 1.5 nt-m. The output response y is shown in figure B. Figure C shows the PMM test determinant values as a function of the assumed model order. The test yielded a model order estimate of 4 for the system. This estimate is based on a threshold used for singularity of PMM. The particular threshold value used in this experiment was found to consistently under estimate the final curve fit model order which in this case is 6. Figure D presents the transfer function spectral estimate $h =_{uy} / P_{uu}$. Transfer function curve fitting on h was performed giving rise to the identified parametric model of Figure E. The identified frequencies and damping coefficients are 0.114 Hz, 0.637 Hz, and 2.75 Hz, and 0.4, 0.0364, and 0.00604, respectively. The frequency values agree well with those of the finite element model of the structure for two axis of rotation as shown in figure 4. Figure F shows the computed output $\hat{y}$ of the identified parametric model subjected to the same excitation input u. Figure G shows the output error $e = y - \hat{y}$, which has a maximum of 2.6 mrad as compared to 10 mrad for y. Finally, the additive uncertainty spectral estimate $\Delta = P_{ue}/P_{uu}$ is shown in figure H. It has a maximum gain value of 11.38 db. Compared with figure D, the value of Δ is 10 db less for the more heavily damped lowest mode, and 29 db less for the two lightly damped higher modes. This indicates that identification of their modal dynamics to within 30% and 10%, respectively, was obtained. Interestingly, there are two modes, apparent in figure D, that were not fitted. Figure H shows that error resulted from omitting those modes is even smaller than the fitting error of the identified modes. This indicates that the curve fitting algorithm has properly determined their omission and produced a reduced-order plant model which minimizes the additive uncertainty. The transfer estimate $\hat{h}$ in figure E, and the additive uncertainty Δ in figure H are now directly usable for robust control design.

6. Conclusions

An automated model order determination and frequency domain identification methodology was presented for the identification and control of large flexible space structures. The product moment matrix approach was used for the estimation of a linear model order to avoid statistical methods which are estimation based, often require processing of large volumes of data, and require major assumptions on the nature of measurement noise. The identification methodology was designed to operate with a high degree of autonomy in an on-orbit environment, and was experimentally verified on a facility designed for emulation of on-orbit testing and control scenarios. The experimental results indicated a close agreement with those of the finite element model of the structure. Furthermore, it demonstrated that the identification algorithm developed produces reduced-order models which minimize a uniform bound on the additive uncertainty. Although the present investigation considered identification of single-input single-output transfer functions, multi-input

Figure 3. Experimental Results using the Autonomous Frequency Domain System Identification Methodology.

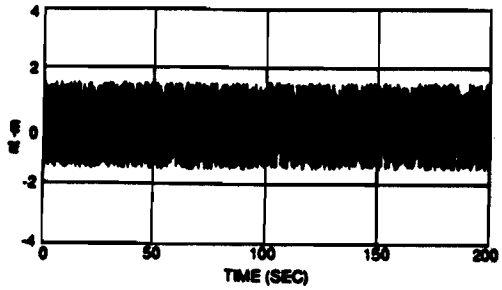

Figure A. Wideband Excitation Input u

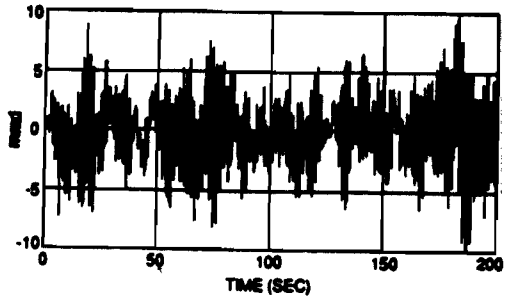

Figure B. Output Response y at Collocated Hub Sensor

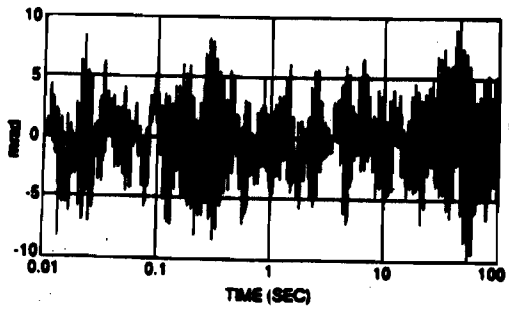

Figure F. Identified Parametric Model Response $\hat{y}$ to Actual Input Excitation

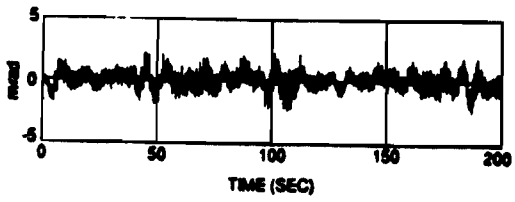

Figure G. Output Error $e = y - \hat{y}$

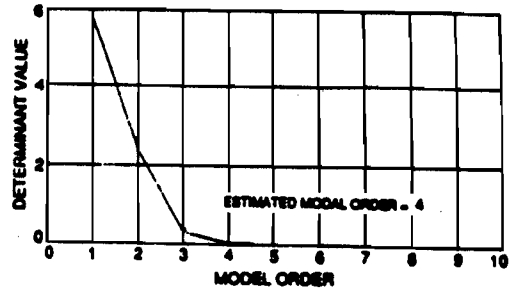

Figure C. PMM Test Determinant Plot

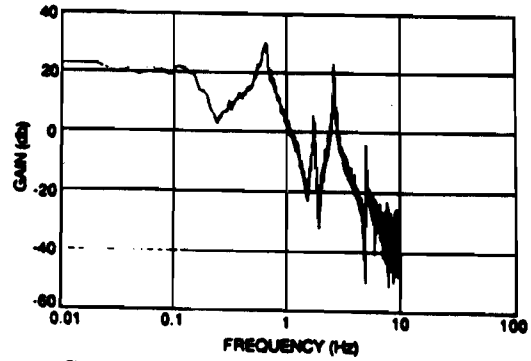

Figure D. Gain Plot of Transfer Function Spectral Estimate h

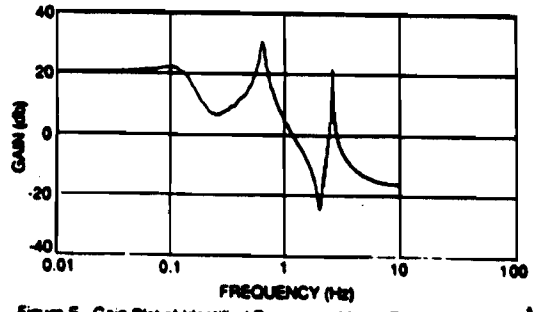

Figure E. Gain Plot of Identified Parametric Model Transfer Function $\hat{h}$

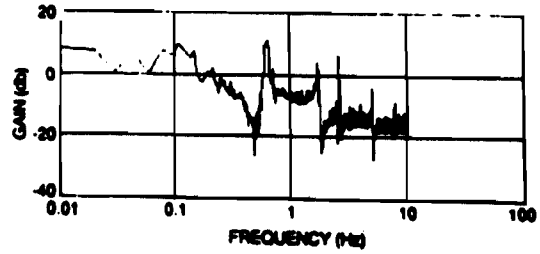

Figure H. Gain Plot of Additive Uncertainty Spectral Estimate $\hat{a}$

Figure 4. Comparison of Finite Element Modeling (FEM) and Experiment Results for Boom-Dish Modal Frequencies.

Axis 1		Axis 2	
FEM Result	Experiment Result	FEM Result	Experiment Result
0.091	0.126	0.091	0.114
0.628	0.666	0.616	0.637
2.682	2.68	2.577	2.57

multi- output system identification would also be accommodated with the present scheme by processing each input-output pair separately.

Acknowledgements

The research described in this paper was performed at the Jet Propulsion Laboratory, California Institute of Technology, under contract with the National Aeronautics and Space Administration.

7. References

1. Soderstrom, T., "On Model Structure Testing in System Identification," Int. J. Control, Vol. 26, No. 1, 1977.

2. Akaike, H., "A New Look at the Statistical Model Identification," IEEE Trans. on Automatic Control, Vol AC-19, No. 6, 1974.

3. Ho, L.R., and Kalman, R.E., "Effective Construction of Linear State-Variable Models from Input-Output Functions," Regelungstechnik 12, 1965.

4. Akaike, H., "Likelihood of a Model and Information Criteria," Journal of Econometrics, Special Issue, 1981.

5. Woodside, C.M., "Estimation of the Order of LInear Systems," Automatica, Vol. 7, 1971.

6. Lee, R.C.K., "Optimal Estimation, Identification and Control," MIT Press, Cambridge, MA, 1964.

7. Soderstrom, T. "Test of Pole-Zero Cancelation in Estimated Models," Automatica, Vol. 11, 1975.

8. Astrom, K.J., "System Identification," Proc. 2nd IFAC Symposium on Identification and Parameter Estimation, 1970.

9. Parzen, E., "A New Look at the Statistical Model Identification," IEEE Trans. on Automatic Control, AC-19, 1974.

10. Yam, Y., et al, "Autonomous Frequency Domain Identification: Theory and Experiment," Jet Propulsion Laboratory, EM 343-1112-89.